JOURNAL OF NATURAL PRODUCTS

Article

Cite This: J. Nat. Prod. XXXX, XXX, XXX−XXX

pubs.acs.org/jnp

NMR-Based Investigation of Hydrogen Bonding in a Dihydroanthracen-1(4*H*)one from *Rubia philippinensis* and Its Soluble Epoxide Hydrolase Inhibitory Potential

Joonseok Oh,[†,‡,#] Khong Trong Quan,[§,⊥,#] Ji Sun Lee,[§] InWha Park,[§] Chung Sub Kim,[†,‡] Daneel Ferreira,[∥] Phuong Thien Thuong,[⊥] Young Ho Kim,[§] and MinKyun Na*[,§]

[†]Department of Chemistry, Yale University, New Haven, Connecticut 06520, United States

[‡]Chemical Biology Institute, Yale University, West Haven, Connecticut 06516, United States

[§]College of Pharmacy, Chungnam National University, Daejeon 34134, Republic of Korea

[⊥]Department of Herbal Analysis and Standardization, National Institute of Medicinal Materials, Hanoi, Vietnam

[∥]Department of BioMolecular Sciences, Division of Pharmacognosy, Research Institute of Pharmaceutical Sciences, School of Pharmacy, The University of Mississippi, University, Mississippi 38677, United States

Supporting Information

ABSTRACT: Hydrogen bonding is a vital feature of a large ensemble of chemical structures. Soluble epoxide hydrolase (sEH) has been targeted for development of the treatment for inflammation-associated diseases. Compounds **1** and **2** were purified from *Rubia philippinensis*, and their structures were established via physical data analysis. Compound **1** possesses intramolecular hydrogen bonding, sufficiently robust to transfer heteronuclear magnetization via a nonbonded interaction. The bonding strength was assessed using the ^{1}H NMR chemical shift temperature coefficients (−1.8 ppb/K), and the heteronuclear coupling constants were measured. The stereochemical details were investigated using interproton distance analysis and ECD. Purified compounds displayed moderate sEH-inhibitory activity.

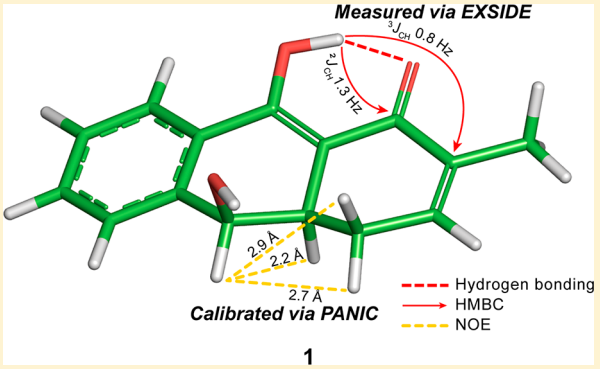

Intermolecular and intramolecular hydrogen-bonding networks are important features of chemical structures and reactivity in drug screening and development.[1] One of the most relevant examples of the former is vancomycin interacting via a series of key intermolecular hydrogen bonding with the D-Ala-D-Ala moieties found in the essential bacterial cell wall precursor lipid II.[2,3] The latter was formed between donor and acceptor functionalities in the same molecule, when molecular configuration and conformation placed them within hydrogen bond geometry.[1] Most drug-like molecules possess a number of functional groups capable of forming these two types of hydrogen bonds, leading ligands to specifically interact with their biomolecular targets.[4] Potential hydrogen bond formation, therefore, should be considered in screening and identification of drug prototypes.[4] Among many approaches for detecting the presence of hydrogen bonding, the NMR method has been recognized as an important tool given its sensitivity for configurational and conformational changes.[5] For instance, temperature coefficients of chemical shifts of hydroxy protons, prone to forming such nonbonding interactions, were obtained via variable-temperature (VT) ^{1}H NMR experiments, and the coefficients were used to evaluate hydrogen-bonding strength.[6] In addition, scalar coupling constants between donors and acceptors involved in intramolecular hydrogen bond formation were directly measurable utilizing several NMR experiments.[5,7]

Soluble epoxide hydrolase (sEH, EC 3.3.2.10) is an enzyme playing a predominant role in hydrolyzing epoxy fatty acids into the related diols in humans and other mammals.[8] The epoxy fatty acids, such as the epoxides of linoleic, arachidonic, eicosatrienoic, and docosahexaenoic acids, are generated by a cytochrome P450-catalyzed oxidation and are endogenous mediators for regulating inflammation,[8] pain,[9] and blood pressure.[10] Thus, elevating levels of endogenous epoxy fatty acids via inhibiting sEH has been validated as a viable strategy for mitigating inflammation and pain[11,12] and lowering blood pressure.[13] During the past few decades, this was substantiated by extensive in vivo studies and clinical trials, and such successes have inspired exploration of sEH inhibitory prototypes for the control of the associated clinical disorders and complications.[14,15] Despite large molecular mass ureas, such as 12-[{(tricyclo[3.3.1.13,7]dec-1-ylamino)carbonyl}-amino]dodecanoic acid (AUDA), exerting powerful sEH inhibitory activity, those scaffolds lack bioavailability due to

Received: June 1, 2018

DOI: 10.1021/acs.jnatprod.8b00441
J. Nat. Prod. XXXX, XXX, XXX−XXX

Table 1. ^{1}H and ^{13}C NMR Spectroscopic Data (600 MHz, 25 °C, DMSO-d_6) for Compounds 1 and 2

	1		2	
position	δ_H, mult. (J in Hz)	δ_C	δ_H, mult. (J in Hz)	δ_C
1		187.6, C	8.55, s	121.4, CH
2		132.6, C		134.3, C
3	6.76, d (6.7)	143.0, CH	7.32, dd (9.0, 1.8)	127.9, CH
4	2.77, m (17.3, 2.8), 2.38, dt (17.3, 6.7)	24.4, CH_2	8.62, d (9.0)	123.5, CH
4a	3.06, ddd (13.6, 6.7, 3.8)	35.3, CH		123.9, C
5	7.41, dd (7.5, 1.1)	129.0, CH	8.69, m	123.5,* CH
6	7.55, td (7.5, 1.1)	132.1, CH	7.44, m	125.0,** CH
7	7.49, td (7.5, 1.1)	128.5, CH	7.44, m	124.7,** CH
8	7.84, dd (7.5, 1.1)	124.4, CH	8.69, m	123.3,* CH
8a		128.9, C		124.4,*** C
9		171.0, C		144.7, C
9a		102.5, C		125.2, C
10	4.46, brt (3.8)	66.5, CH		146.4, C
10a		141.1, C		125.4,*** C
11	1.82, brq (1.2)	15.5, CH_3	2.50, overlap	21.9, CH_3
9-OH	16.07, s[a]			
10-OH	5.19, d (4.4)[a]			
9-*O*-glucopyranosyl				
1′			4.85, d (7.8)	106.0
2′			3.59, d (7.8)	74.4
3′			3.30, overlapped	76.5
4′			3.30, overlapped	69.8
5′			3.00, m	76.8
6′			3.49, dd (11.5, 1.8)	61.0
			3.42, dd (11.7, 4.8)	
10-*O*-glucopyranosyl				
1″			4.86, d (7.8)	106.0
2″			3.61, d (7.8)	74.5
3″			3.30, overlapped	76.5
4″			3.30, overlapped	69.8
5″			3.00, m	76.8
6″			3.52, dd (11.5, 1.8)	61.1
			3.41, dd (11.4, 4.8)	

[a]Chemical shift values depending on various temperatures in acetone-d_6 are available in Figures S10−S12, Supporting Information. *, **, ***Values within each column may be interchanged.

limited solubility in both water and organic solvents, which has prompted a continuing search for potential chemical scaffolds capable of inhibiting the target hydrolase.

In an ongoing phytochemical study aimed at the identification of bioactive secondary metabolites from *Rubia philippinensis* Elmer (Rubiaceae), compounds **1** and **2** were identified via a combinatorial approach of computation with conventional and advanced NMR techniques. VT ^{1}H NMR studies ranging in temperature from 200 to 300 K permitted the identification of intramolecular hydrogen bonding in **1**. Interestingly, this nonbonding interaction was sufficiently robust to generate nonbonding scalar heterocoupling constants ($^{2}J_{C\text{-}1,OH}$ and $^{3}J_{C\text{-}2,OH}$), which were directly measured using the excitation-sculptured indirect-detection experiment (EXSIDE).[16] The configurational analysis was carried out utilizing comparison of experimental and simulated electronic circular dichroism (ECD) spectra. These anthracene-type compounds were also evaluated for their sEH inhibitory potential.

RESULTS AND DISCUSSION

Compound **1** was obtained as a yellow powder. The protonated HRESIMS ion detected at m/z 243.1022 along with the ^{13}C NMR data (Table 1) established the molecular formula of **1** as $C_{15}H_{14}O_3$ (calcd $[M + H]^+$, m/z 243.1021; Figure S1, Supporting Information). The ^{1}H NMR data indicated characteristic resonances for four aromatic methines (δ_H 7.41, 7.49, 7.55, 7.84), an olefinic proton (δ_H 6.76), an oxygenated methine (δ_H 4.46), a methine (δ_H 3.06), a methylene (δ_H 2.77, 2.38), and an allylic methyl motif (δ_H 1.82). The ^{13}C and DEPT135 NMR data exhibited 15 carbons, including an α,β-unsaturated carbonyl moiety (δ_C 187.6, 102.5, 171.0) and six aromatic and two olefinic carbons, together with an oxygenated methine, a methine, and a methylene carbon. Comparison of its ^{1}H and ^{13}C NMR data with rubiasin A from *R. cordifolia*[17] suggested that **1** is a dihydroanthracen-1(4*H*)one-type molecule. This was confirmed via the COSY correlations between H-3/H_2-4, H-4/H-4a, and H-4a/H-10 (Figure 1). The HMBC cross-peaks of H_3-11 (δ_H 1.82) and H-3 (δ_H 6.76) with C-1 (δ_C 187.6) placed the ketocarbonyl functionality at C-1, while HMBC cross-peaks of H-5 (δ_H 7.41) with C-10 (δ_C 66.5), H-4 (δ_H 2.77, 2.38) with C-2 (δ_C 132.6), and H_3-11 (δ_H 1.82) with C-2 established the locations of the hydroxy and methyl groups at C-10 and C-2, respectively. Interestingly, a highly deshielded hydroxy proton resonance (δ_H 16.07) was observed in multiple ^{1}H NMR experiments using variable spectrum widths and anhydrous

DOI: 10.1021/acs.jnatprod.8b00441
J. Nat. Prod. XXXX, XXX, XXX−XXX

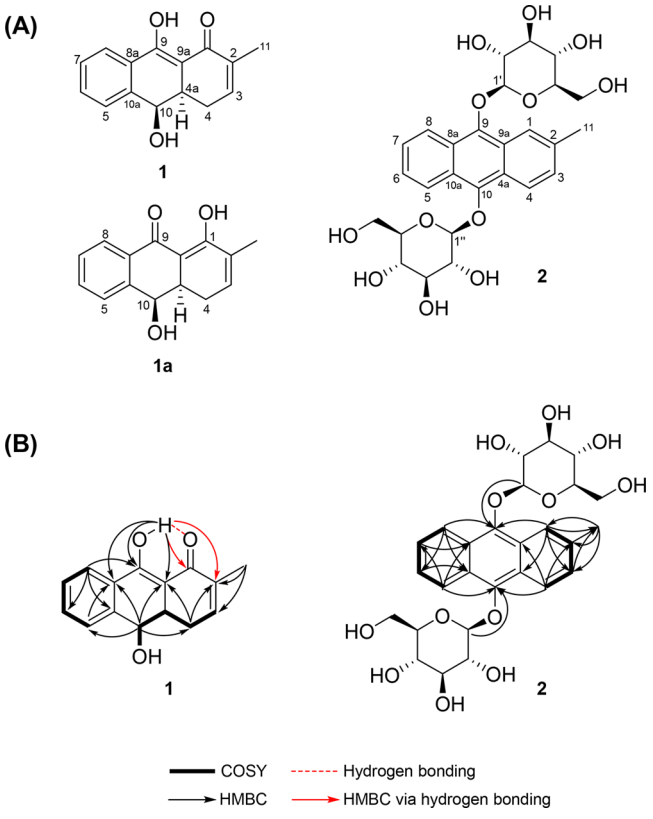

Figure 1. (A) 2D structures of compounds **1** and **2** and (B) key 2D NMR correlations. The respective 2D correlations from hydroxy protons were detected in anhydrous acetone-d_6 or DMSO-d_6.

aprotic NMR solvents (DMSO-d_6 or acetone-d_6) (Figure 2 and Figures S2 and S12, Supporting Information). This suggests that the exchangeable proton is involved in strong intramolecular hydrogen bonding. The hydroxy proton displayed HMBC cross-peaks to C-9 (δ_C 171.0), C-9a (δ_C 102.5), and C-8a (δ_C 128.9), as shown in Figure 1, rendering the deshielded proton to be assigned tentatively to HO-9 (Figure 1). The deshielded proton, however, also displayed HMBC cross-peaks with the carbonyl carbon (δ_C 187.6) and C-2 (δ_C 132.6) (Figure 1B). It was speculated initially that keto−enol tautomerism involving the β-hydroxyenone functionality might lead to the generation of such heteronuclear NMR correlations on the NMR time scale. To verify this assumption, VT ^{1}H NMR experiments (200 to 300 K, acetone-d_6, 10 mM) were conducted in an attempt to observe the footprints of each tautomer.[18] However, based on the resultant NMR spectra (Figure 2 and Figures S10−S12, Supporting Information), such an interconversion apparently does not occur. Alternatively, a temperature coefficient [$\Delta\delta/\Delta T$(K)] of the hydroxy proton was calculated to evaluate its hydrogen-bonding strength since heteronuclear couplings from an exchangeable hydrogen atom to heteroatoms (i.e., ^{13}C, ^{15}N, or ^{121}Sb and ^{123}Sb) were feasible via localized hydrogen bonding.[5−7,19] The temperature coefficient of the hydroxy proton in acetone-d_6 was −1.8 ppb/K (200 to 300 K, acetone-d_6, 10 mM; Figure 2), much stronger than those measured for the hydrogen bonds between HO-5 and the ketocarbonyl moieties in the flavonols kaempferol (−3.1 ppb/K) and quercetin (−2.9 ppb/K) and the flavone luteolin (−2.3 ppb/K) under similar VT NMR experimental conditions.[6] This evidenced the presence of a robust intramolecular hydrogen bonding from HO-9 (δ_H 16.07) to the C-1 carbonyl oxygen, transferring magnetization from the hydroxy proton to C-1 and C-2 in the HMBC experiment even with routine heteronuclear transfer delay and coupling constant settings ($^nJ_{CH}$ = 8 Hz; Figure 1 and Figure S7, Supporting Information). The long-range heteronuclear coupling constants were measured utilizing EXSIDE to confirm $^2J_{C\text{-}1,OH}$ (1.3 Hz) and $^3J_{C\text{-}2,OH}$ (0.8 Hz) values (Figure 3). The ^{13}C NMR chemical shift of C-1 along with the respective heterocoupling constants from HO-9 to C-8a (4 Hz), C-9 (4 Hz), and C-9a (5 Hz) (Figures S13−S15, Supporting Information), larger than those via the hydrogen bonding,[7] confirmed the presence of the 4a,10-dihydroanthracen-1(4*H*)-one (**1**) rather than a 4a,10-dihydroanthracen-9(4*H*)-one (**1a**) motif (Figure 1). Collectively, these criteria defined the 2D structure of **1** as shown in Figure 1.

The relative configuration was established based upon the homonuclear coupling constant $^3J_{H\text{-}4a,H\text{-}10}$ (3.8 Hz) and NOE-derived interproton distances from H-10 to H-4a and the diastereotopic protons H_2-4. To accomplish the configurational analysis via accurate interproton distances, the 1D NOESY sequence based on the double-pulse field gradient spin−echo NOE pulse and the peak amplitude normalization for improved cross-relaxation (PANIC) method were employed (Figure 4 and Figures S16 and S17, Supporting Information).[20,21] The PANIC-based calibrated interproton distances from H-10 to H-4a, H-4α, and H-4β were 2.2, 2.7, and 2.9 Å, respectively. These spatial distances exhibited an excellent agreement with those simulated for a diastereomer of **1** possessing a (4a*R**,10*R**) configuration. For the establishment of the absolute configuration of **1**, Mosher's method[22] was initially attempted. Unlike the identical approach used for rubiasin A,[17] only the *S*-MTPA derivative could be formed (Figure S18, Supporting Information). Alternatively, the absolute configurational assignment was done via comparison of the experimental and simulated ECD spectra. As shown in Figure 5, both experimental and computed ECD spectra exhibited the respective negative and positive Cotton effects at ca. 250 and 280 nm originating from the UV bands of the dihydroanthracen-1(4*H*)one architecture.[17] Ultimately, the full structure of **1** was established as (4a*R*,10*R*)-9,10-dihydroxy-2-methyl-4a,10-dihydroanthracen-1(4*H*)-one.

The HRESIMS analysis of **2** (yellowish, amorphous powder) exhibited a sodium-adduct ion at *m*/*z* 571.1787 (Figure S20, Supporting Information), and the molecular formula was assigned as $C_{27}H_{32}O_{12}$ in conjunction with the ^{13}C NMR data (Table 1). The 1D NMR data of **2** shared close similarities with those of typical 9,10-anthraquinones except for the presence of the ^{13}C NMR resonances for two oxygenated aromatic tertiary carbons (δ_C 144.7, 146.4) and the absence of two ketocarbonyl functionalities (ca. δ_C 180). This is indicative of the two ketocarbonyl functionalities being reduced to the corresponding phenolic moieties, which was confirmed by the respective HMBC cross-peaks from H-1, H-8 and H-4, H-5 to C-9 and C-10 (Figure 1). The C-2 methyl motif was determined via the HMBC cross-peaks from H-1 and H-3 to the methyl carbon and from H_3-11 to C-1, C-2, and C-3 (Figure 1). The HMBC cross-peaks of the H-1′ and H-1″ anomeric protons (δ_H 4.85, 4.86) with the oxygenated aromatic tertiary carbons (δ_C 144.7, 146.4) established the locations of the monosaccharide moieties at C-9 and C-10. The large coupling constants of the anomeric protons (*J* = 7.8 Hz) both indicated β-glucosidic linkages. The D-configuration of the glucopyranose moieties was established using chiral

DOI: 10.1021/acs.jnatprod.8b00441
J. Nat. Prod. XXXX, XXX, XXX−XXX

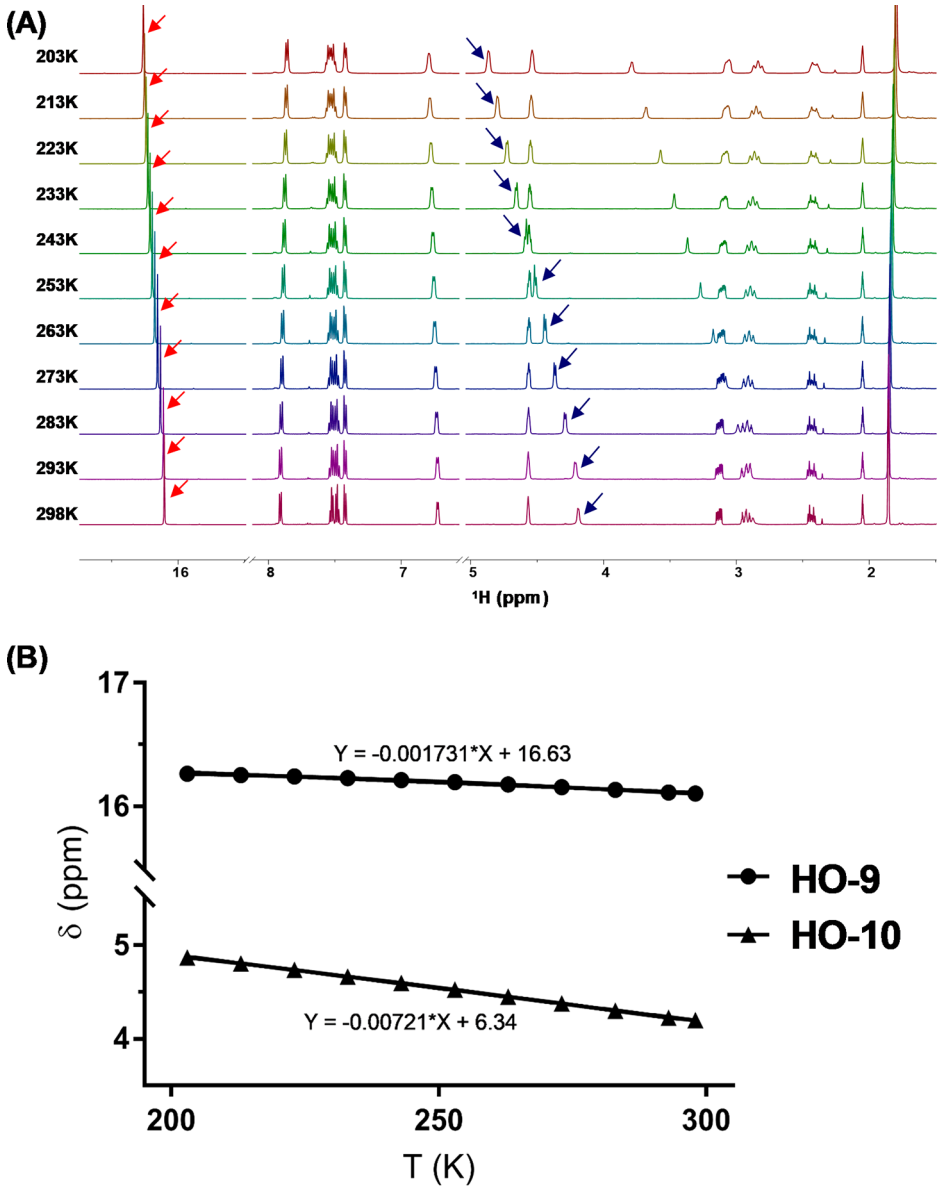

Figure 2. (A) VT ^{1}H NMR experiments of **1** (200−300 K, acetone-d_6; HO-9 and HO-10 are indicated in red and blue, respectively) and (B) temperature coefficients of the two hydroxy protons HO-9 (−1.8 ppb/K) and HO-10 (−7.3 ppb/K) (10 mM). Some ranges for the stacked ^{1}H NMR spectra were snipped for better presentation. Another labile proton resonating at 3−4 ppm throughout the VT experiments is HDO.[26]

derivatization followed by LC analyses (Figure S26, Supporting Information).[23] Consequently, the structure of **2** was established as 9,10-di-*O*-*β*-D-glucopyranosyl-2-methylanthracene.

The purified compounds were tested for their inhibitory potential against sEH and exhibited inhibition with IC_{50} values of 1.1 and 0.3 μM, respectively. These inhibitory activities are relatively moderate in comparison with the positive control AUDA (IC_{50} 0.6 nM); however, **1** and **2** might be employed for the generation/expansion of chemical libraries to implement preliminary lead optimization and SAR studies for the development of sEH inhibitors, given the interesting scaffold possessing robust hydrogen bonding and observed inhibitory activity.

EXPERIMENTAL SECTION

General Experimental Procedures. Optical rotations were obtained on a JASCO DIP-1000 automatic digital polarimeter (Tokyo, Japan), IR data were generated on a Thermo Electron US/Nicolet380 (Madison, WI, USA), and ECD spectra were recorded on a Chirascan qCD (Applied Photophysics, UK). NMR experiments were performed on a Bruker Avance III (600 MHz) spectrometer (Billerica, MA, USA). HRESIMS data were generated on a Waters SYNAPT G2 high-resolution mass spectrometer (Milford, MA, USA). The VT experiments were conducted by cooling the probe using liquid N_2. TLC was performed on glass plates precoated with silica gel 60 F254 or RP-18 F254 (20 × 20 cm, 200 μm, 60 Å, Merck, Kenilworth, NJ, USA). Vacuum-liquid chromatography (VLC) was conducted on Merck silica gel (70−230 mesh), and MPLC was carried out using a Biotage Isolera equipped with a reversed-phase C_{18} SNAP Cartridge KPC18-HS (120 or 400 g, Uppsala, Sweden). HPLC was performed on a Gilson system (Middleton, WI, USA) with a Phenomenex Kinetex 5 μm C_{18} column (250 × 21.20 mm, 5 μm, Torrance, CA, USA).

Plant Material. The roots of *R. philippinensis* were collected from Bidoup-Nui Ba National Park, Lamdong Province, Vietnam, in August 2014, and identified by two of the authors, P.T.T. and M.N. A voucher specimen was deposited at the herbarium of the Vietnam

DOI: 10.1021/acs.jnatprod.8b00441
J. Nat. Prod. XXXX, XXX, XXX−XXX

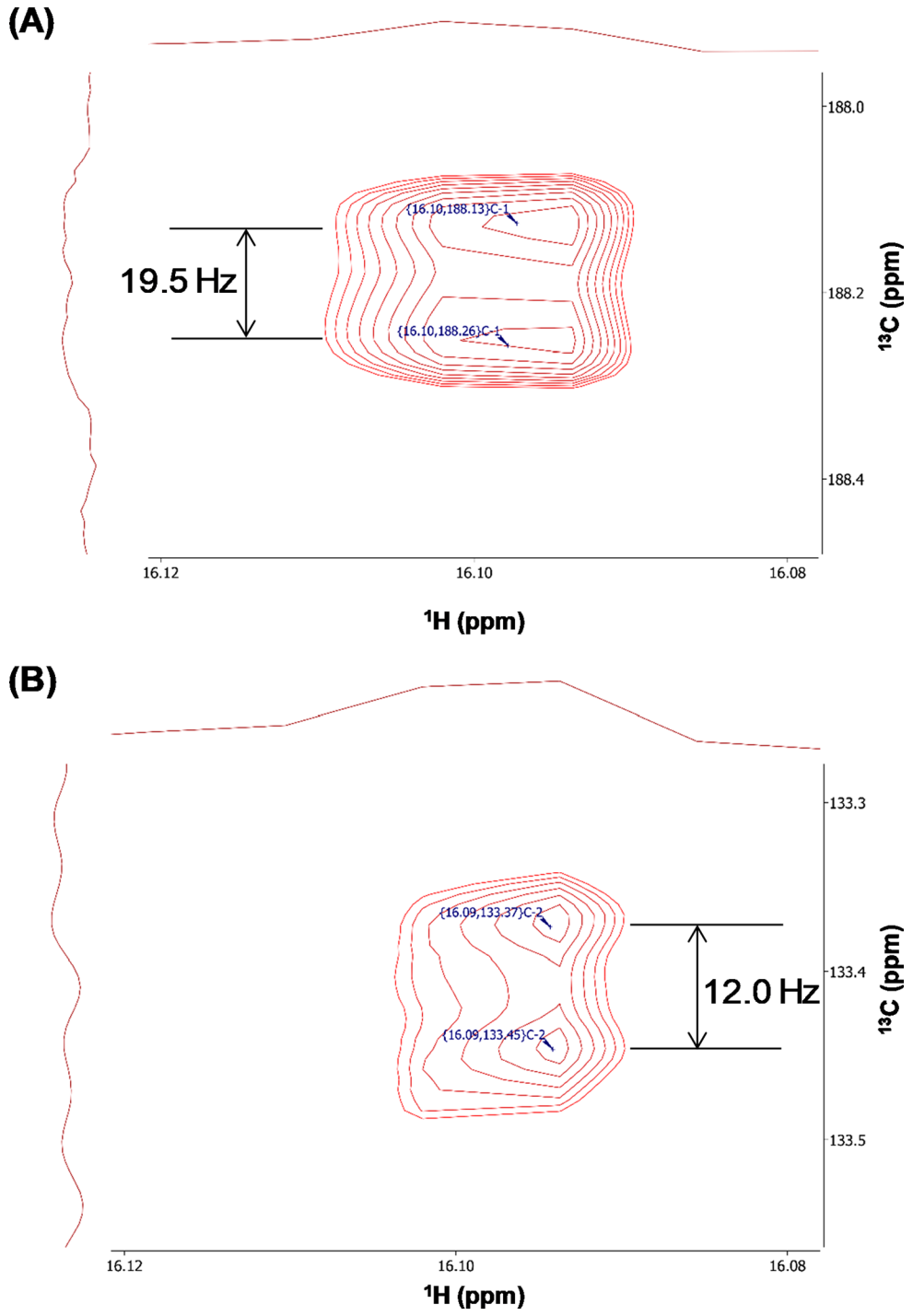

Figure 3. Heteronuclear coupling constants for HO-9 to C-1 ($^2J_{C\text{-}1,OH}$ = 1.3 Hz) (A) and to C-2 ($^3J_{C\text{-}2,OH}$ = 0.8 Hz) obtained from EXSIDE spectra, where those values were acquired via dislocation in Hz along with the f1 dimension divided by the scaling factor 15. See the Experimental Section for details regarding the NMR parameters.

National Institute of Medicinal Materials, Hanoi, Vietnam (VDL20140801), as well as the Laboratory of Pharmacognosy at the College of Pharmacy, Chungnam National University, Daejeon, Korea (CNU1409).

Extraction and Isolation. The dried roots of *R. philippinensis* (1.5 kg) were extracted with EtOH (3 L × 3) at room temperature for 4 days. The crude extract was concentrated under vacuum to yield a reddish-brown slurry (150 g). The slurry was suspended in H_2O (1.5 L) and sequentially partitioned with CH_2Cl_2 (3 × 2 L) and EtOAc (3 × 2 L) to yield the CH_2Cl_2, EtOAc, and H_2O extracts. The CH_2Cl_2 fraction (50 g) was subjected to silica gel VLC and eluted with *n*-hexane/EtOAc (20:1, 10:1, 5:1, 3:1, 2:1) and $CHCl_3$/MeOH (8:1) to yield six fractions (D-1−D-6). Fraction D-4 (6.1 g) was divided into 10 subfractions (D-4−1−D-4−10) using MPLC (column size 400 g) with a gradient of MeOH/H_2O (10:90 → 100:0, 7 L). Fractions D-4-2 (180 mg) and D-4-3 (120 mg) were purified utilizing MeOH/H_2O (60:40, 4 mL/min, UV 254 nm) to yield **1** (t_R 37.0 min, 10 mg). The EtOAc fraction (14.0 g) was subjected to silica gel VLC and eluted with *n*-hexane/EtOAc/MeOH (2:1:0.2) and $CHCl_3$/MeOH (8:1, 5:1, 3:1, 0:1) to produce five fractions (EA-1−EA-5). Fraction EA-4 (2.6 g) was divided into 11 subfractions (EA-4-1−EA-4-11) using MPLC (column size 120g) with a gradient of MeOH/H_2O (10:90 →

DOI: 10.1021/acs.jnatprod.8b00441
J. Nat. Prod. XXXX, XXX, XXX−XXX

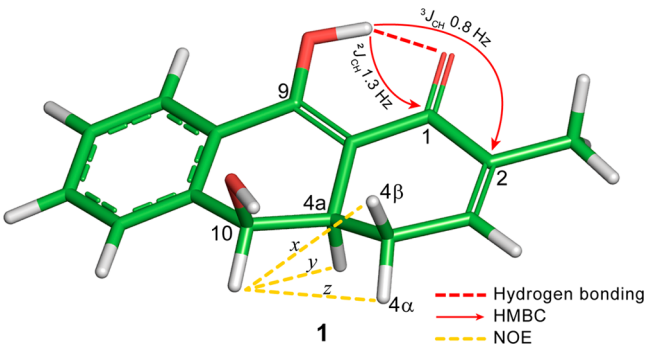

Figure 4. HMBC via the intramolecular hydrogen bonding from HO-9 and quantitative NOE-distance measurement for relative configurational analysis of **1**. NOE-derived interproton distances are denoted with their respective predicted distances shown in parentheses: x = 2.9 Å (3.1 Å); y = 2.2 Å (2.3 Å); z = 2.7 Å (2.7 Å). The 3D structure was optimized at the B3LYP/6-31+G(d,p) level in the PCM mode (CH_3CN).

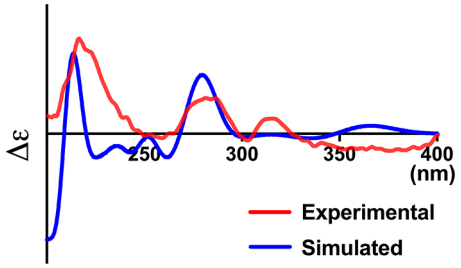

Figure 5. Overlay of experimental and simulated ECD spectra of compound **1**. The simulation was carried out at the B3LYP/6-31+G(d,p) level in the PCM mode (CH_3CN).

100:0, 5 L). Compound **2** (20 mg) was obtained from fraction EA-4-3 (51 mg) employing HPLC, eluting with MeOH/H_2O (40:60, 2.5 mL/min, UV 254 nm, t_R 40.6 min).

Enzymatic Hydrolysis of 2 and Establishment of the Absolute Configuration of Sugar Moieties. Compound **2** (2 mg) was treated with β-glucosidase from almonds (5 mg; Sigma-Aldrich, St. Louis, MO, USA) in 1 mL of distilled H_2O at 37 °C for 20 h. The mixtures were passed through filters (PTFE 0.45 μM) to obtain the aqueous solutions containing the resultant monosaccharides. The solutions were dried and subjected to chiral derivatization.[23] The sugar-containing residue was dissolved in pyridine (0.5 mL) containing L-cysteine methyl ester hydrochloride (3 mg) and heated at 60 °C for 1 h. Phenyl isothiocyanate (50 μL) was added, and the mixtures were heated at 60 °C for another 1 h. The reaction mixture was dried under a stream of N_2 gas to remove residual pyridine. The residue was dissolved in 1 mL of HPLC-grade MeOH and analyzed employing an LC-10AD series HPLC system (Shimadzu, Kyoto, Japan) equipped with a Phenomenex column (250 × 4.6 mm, 5 μm), mobile phase CH_3CN/H_2O (25:75) with a flow rate of 0.6 mL/min. The sample solution (10 μL) was injected onto the system, and the derivatized sugar moiety was detected at the UV wavelength 250 nm. Authentic D- and L-glucopyranose (each 1 mg) were derivatized and analyzed using the identical protocol. The D-configuration of the sugar motif was established based upon the comparison of the retention time of the sugar derivative of **2** (t_R 15.398 min) with those of the standard D-glucose (t_R 15.391 min) and L-glucose (t_R 14.596 min) derivatives (Figure S26, Supporting Information).

Compound 1: yellow, viscous oil; $[\alpha]_D^{22}$ +236 (c 0.2, MeOH); UV (MeOH) λ_{max} (log ε) 246 (4.08), 372 (4.12) nm; IR (neat) ν_{max} 3382, 1668, 1615, 1595, 1557, 1284, 1065, 1047, 758 cm^{-1}; ^1H and ^{13}C NMR, see Table 1; HRESIMS m/z 265.0837 $[M + Na]^+$, m/z 243.1022 $[M + H]^+$ (calcd for $C_{15}H_{14}O_3Na$, 265.0841, and $C_{15}H_{15}O_3$, 243.1021).

Compound 2: yellowish, amorphous powder; $[\alpha]_D^{22}$ −175 (c 0.3, MeOH); UV (MeOH) λ_{max} (log ε) 219 (4.59), 247 (4.73), 358 (4.17), 376 (4.29), 397 (4.24) nm; IR (neat) ν_{max} 3349, 1058, 1018 cm^{-1}; ^1H and ^{13}C NMR, see Table 1; HRESIMS m/z 571.1787 $[M + Na]^+$ (calcd for $C_{27}H_{32}O_{12}Na$, 571.1791).

Parameters for EXSIDE and PANIC.[20,21] The key EXSIDE NMR experiment was carried out using the Bruker pulse hsqcetgplrjcsp with t1 increments (indirect dimension) of 900 and a scaling factor of 15, to ensure sufficient resolution to observe splitting of correlations along the f1 dimension. According to the original author's recommendation,[16] a selective pulse width (i.e., the HO-9 resonance in this study) for the direct dimension (f2) should be carefully chosen as wide as possible to shorten the relaxation delay for a generated shaped pulse. To increase the digital resolution, the f1 spectrum width was reduced to ∼100 ppm. The 1D NOESY for the PANIC analysis was implemented using a double-pulse field gradient spin−echo NOE (DPFGSENOE) excitation sculpted selective sequence incorporated with a zero-quantum filter element (500 ms mixing time, 2 s relaxation time, 64 scans). The equation below was utilized to acquire accurate interproton distances ("$r_{unknown}$"). The resonance for H-8 in compound **1** was selectively irradiated using 1D NOESY, and the integration for the irradiated resonance was arbitrarily normalized to −1000. The generated NOE intensity for H-7 was integrated with reference to −1000 (Figure S16, Supporting Information), and the integration of H-7 was used as "$NOE_{reference}$". The typical interproton distance between the aromatic protons (i.e., H-7 to H-8) of 2.5 Å was used as "$r_{reference}$". To calibrate interproton distances from H-10 to H-4a and from H-4α to H-4β ("$r_{unknown}$"), H-10 was irradiated using the aforementioned pulse. Its integration was normalized to −1000, and the resultant NOE integrations for H-4a and the two diastereotopic protons (Figure S17, Supporting Information) were used to obtain respective "$r_{unknown}$" values with the following equation.

$$NOE_{unknown}/NOE_{reference} = (r_{reference})^6/(r_{unknown})^6$$

Computational Details. All conformers of **1** were identified using the Macromodel (version 2015-2, Schrodinger LLC) module with "mixed torsional/low mode sampling" in the MMFF94 force field. The search process was initially performed in the gas phase with a 50 kJ/mol energy window limit and 10 000 maximum number of steps to identify all potential conformers. The Polak−Ribiere conjugate gradient protocol was utilized to minimize conformers with 10 000 maximum iterations and a 0.001 kJ $(mol\ Å)^{-1}$ convergence threshold on the rms gradient. Two conformers were found within 10 kJ/mol of each global minimum and subjected to geometry optimization using the Gaussian 09 package (Gaussian Inc.) at the B3LYP/6-31+G(d,p) level with the polarizable continuum model (PCM) mode with a dielectric constant representing CH_3CN. The optimized coordinates were utilized for ECD simulation at the identical functional basis set, and the Boltzmann-averaged spectrum was visualized using SpecDis.[24] The interproton distance analysis for the establishment of the relative configuration of **1** was performed using the most abundant conformers of each plausible diastereomer (i.e., 4a*R**,10*R** and 4a*S**,10*R**) at the aforementioned basis set. In the epimer (4a*S**,10*R*), the predicted distances from H-10 to H-4a, H-4α, and H-4β were 3.0, 3.0, and 2.4 Å.

sEH Assay. The assay was conducted with reference to a published protocol.[25] A 50 μL amount of sEH (140 ng/mL) and 20 μL of different concentrations of compounds **1** and **2** in MeOH were mixed in a 96-white-well plate containing 80 μL of 25 mM bis-Tris-HCl buffer (pH 7.0) and 0.1% bovine serum albumin. The mixture was incubated at 37 °C, and the products of hydrolysis were monitored at excitation and emission wavelengths of 330 and 465 nm after 1 h.

DOI: 10.1021/acs.jnatprod.8b00441
J. Nat. Prod. XXXX, XXX, XXX−XXX

■ ASSOCIATED CONTENT

Supporting Information

The Supporting Information is available free of charge on the ACS Publications website at DOI: 10.1021/acs.jnatprod.8b00441.

1D and 2D NMR and HRESIMS spectra of **1** and **2**, VT experiments of **1**, and computational details (PDF)

■ AUTHOR INFORMATION

Corresponding Author

*Tel: +82 42 821 5925. Fax: +82 42 823 6566. E-mail: mkna@cnu.ac.kr (M. Na).

ORCID

Chung Sub Kim: 0000-0001-9961-4093
Daneel Ferreira: 0000-0002-9375-7920
Young Ho Kim: 0000-0002-5212-7543
MinKyun Na: 0000-0002-4865-6506

Author Contributions

#J. Oh and K. T. Quan contributed equally.

Notes

The authors declare no competing financial interest.

■ ACKNOWLEDGMENTS

This study was supported by the Basic Science Research Program (NRF-2017R1A2A2A05001340) through the National Research Foundation of Korea (NRF) grant funded by the Korean Government. This work was also supported by the Korea Polar Research Institute (grant no. PE18210). We thank Drs. E. Kwan (Harvard University), C. P. Butts (University of Bristol), K. Krishnamurthy (Chempacker LLC), and Agilent Spinsights Forum for practical advice regarding NMR techniques used in this study. We also recognize the Korea Institute of Science and Technology Information (KISTI) for supercomputing access.

■ REFERENCES

(1) Jeffrey, G. A.; Saenger, W. *Hydrogen Bonding in Biological Structures*; Springer-Verlag: Berlin, 1991.
(2) Yim, G.; Thaker, M. N.; Koteva, K.; Wright, G. *J. Antibiot.* **2014**, *67*, 31−41.
(3) Butler, M. S.; Hansford, K. A.; Blaskovich, M. A.; Halai, R.; Cooper, M. A. *J. Antibiot.* **2014**, *67*, 631−644.
(4) Kuhn, B.; Mohr, P.; Stahl, M. *J. Med. Chem.* **2010**, *53*, 2601−2611.
(5) Huang, X. S.; Liu, X.; Constantine, K. L.; Leet, J. E.; Roongta, V. *Magn. Reson. Chem.* **2007**, *45*, 447−450.
(6) Exarchou, V.; Troganis, A.; Gerothanassis, I. P.; Tsimidou, M.; Boskou, D. *Tetrahedron* **2002**, *58*, 7423−7429.
(7) Borisov, E.; Zhang, W.; Bolvig, S.; Hansen, P. E. *Magn. Reson. Chem.* **1998**, *36*, S104−S110.
(8) Morisseau, C.; Hammock, B. D. *Annu. Rev. Pharmacol. Toxicol.* **2013**, *53*, 37−58.
(9) Kitamura, S.; Morisseau, C.; Inceoglu, B.; Kamita, S. G.; De Nicola, G. R.; Nyegue, M.; Hammock, B. D. *PLoS One* **2015**, *10*, e0117438.
(10) Lin, W.-K.; Falck, J.; Wong, P. Y. *Biochem. Biophys. Res. Commun.* **1990**, *167*, 977−981.
(11) Inceoglu, B.; Jinks, S. L.; Schmelzer, K. R.; Waite, T.; Kim, I. H.; Hammock, B. D. *Life Sci.* **2006**, *79*, 2311−2319.
(12) Rose, T. E.; Morisseau, C.; Liu, J.-Y.; Inceoglu, B.; Jones, P. D.; Sanborn, J. R.; Hammock, B. D. *J. Med. Chem.* **2010**, *53*, 7067−7075.
(13) Imig, J. D.; Zhao, X.; Capdevila, J. H.; Morisseau, C.; Hammock, B. D. *Hypertension* **2002**, *39*, 690−694.
(14) Https://clinicaltrials.gov/ct2/show/NCT00847899?term=NCT00847899.&rank=1, accessed on July 15, 2015.
(15) Imig, J. D.; Hammock, B. D. *Nat. Rev. Drug Discovery* **2009**, *8*, 794−805.
(16) Krishnamurthy, V. *J. Magn. Reson., Ser. A* **1996**, *121*, 33−41.
(17) Chang, L. C.; Chávez, D.; Gills, J. J.; Fong, H. H. S.; Pezzuto, J. M.; Kinghorn, A. D. *Tetrahedron Lett.* **2000**, *41*, 7157−7162.
(18) Sečkářová, P. N.; Marek, R.; Maliňáková, K.; Kolehmainen, E.; Hocková, D.; Hocek, M.; Sklenář, V. *Tetrahedron Lett.* **2004**, *45*, 6259−6263.
(19) Tokunaga, T.; Seki, H.; Yasuike, S.; Ikoma, M.; Kurita, J.; Yamaguchi, K. *Tetrahedron Lett.* **2000**, *41*, 1031−1034.
(20) Butts, C. P.; Jones, C. R.; Song, Z.; Simpson, T. J. *Chem. Commun.* **2012**, *48*, 9023−9025.
(21) Hu, H.; Krishnamurthy, K. *J. Magn. Reson.* **2006**, *182*, 173−177.
(22) Hoye, T. R.; Jeffrey, C. S.; Shao, F. *Nat. Protoc.* **2007**, *2*, 2451−2458.
(23) Tanaka, T.; Nakashima, T.; Ueda, T.; Tomii, K.; Kouno, I. *Chem. Pharm. Bull.* **2007**, *55*, 899−901.
(24) Bruhn, T.; Hemberger, Y.; Schaumloffel, A.; Bringmann, G. *SpecDis*, Version 1.51; University of Wuerzburg: Germany, 2011.
(25) Jones, P. D.; Wolf, N. M.; Morisseau, C.; Whetstone, P.; Hock, B.; Hammock, B. D. *Anal. Biochem.* **2005**, *343*, 66−75.
(26) Gottlieb, H. E.; Kotlyar, V.; Nudelman, A. *J. Org. Chem.* **1997**, *62*, 7512−7515.

DOI: 10.1021/acs.jnatprod.8b00441
J. Nat. Prod. XXXX, XXX, XXX−XXX